Analysis of nervous fiber, muscle, and blood vessels using their ulraviolet near infrared reflectance characteristics

Kadir Tufan[a,*] and Ahmet Korkut Belli[b]
[a]Computer Engineering Department, Fatih University, Istanbul, Turkey
[b]Department of General Surgery, Mugla Sitki Kocman Medical School, Mugla, Turkey

Abstract. Injury to the nervous system can lead to irreversible problems as nervous tissues have limited regenerative capability. Therefore it is imperative to find an objective, reliable, cheap, and easy-to-apply method that separates nervous fibers from muscles and blood vessels. The aim of this study is to determine structural differences that can aid in easy and reliable identification of nervous fibers. We analyzed light reflectance from these tissues from 230 nm to 1000 nm and found that in the range of 400 nm-600 nm nervous fibers have higher reflectance in comparison to others. Therefore, we generated distinct features in this range and utilized support vector machine to automatically classify samples. Classification performance demonstrated that light reflectance is a good candidate feature that can help to classify nervous tissue.

Keywords: Nervous tissue, light reflectance, surgery, support vector machines

1. Introduction

The nervous system (NS) is the signal carrier in human and animals [1], which coordinates the actions of different parts of the body by transmitting signals. These actions can be classified as voluntary or involuntary [2]. The central nervous system (CNS) and peripheral nervous system (PNS) are the two components of the NS. The brain and spinal cord make up the CNS [3], whereas the PNS includes the motor (voluntary) or autonomic (involuntary) actions of the body. PNS fibers carry sensory signals like pressure, temperature, and pain to the CNS and also send commands (motor actions) from the CNS to the target organs [4].

Injury to the NS is different from any other injury because the NS does not have regenerative capability [5, 6]. Due to this limitation, any damage to the NS is permanent and lasts for the rest of a person's life [7, 8]. Surgery carries the risk of damaging nervous fibers. Iatrogenic trauma is defined as the injuries caused by a healthcare provider during a surgical procedure. Therefore, it is very important during surgery to differentiate nervous fibers from similar tissues, such as blood vessels and muscle fibers etc. Unfortunately, there are limited solutions suggested in the literature for this critical issue [7-9].

---

* Address for correspondence: Kadir Tufan, Chairman of Computer Engineering Department, Fatih University, 34500, Buyukcekmece, Istanbul, Turkey. Tel.: +90 212 866 33 00; Fax: +90 212 866 34 12; E-mail: ktufan@fatih.edu.tr.

Table 1

Numbers and place of sample collection

Sample Name	Number of Samples	Place of collection
Nervous Fiber	40	Main nerve of the hind leg
Muscle	40	Hind leg muscle
Blood Vessel	40	Main vein of the hind leg

The surgeon's anatomic knowledge during an operation is his/her primary aid for correctly distinguishing nervous fibers. The stiffer and tenser form of the nervous fiber can also be used as a guide during open surgery. However, the surgeon's sense of touch cannot be utilized during a closed operation. Radiological imaging methods are also useful but the practical application of radiologic imaging is very weak during surgery [10]. A more practical suggestion called electrophysiological nerve monitoring (EPNM) is suggested and available for thyroid surgery or some otologic procedures, despite the fact that it has to include the presence of an electrophysiological expert during each surgery [11-13]. The need for an objective, easy-to-apply, and reliable tool for the differentiation of nervous fibers during surgery has not been accomplished.

Methods that utilize the structural characteristics of nervous fibers can be extremely useful. In this study, the ultraviolet near infrared (UV-NIR) light reflectance of nervous fibers, blood vessels, and muscle tissues acquired from cows are investigated. Here, we have analyzed the samples by using a UV-NIR spectrophotometer (UV-NIR-SPM). A support vector machine (SVM) is then used to classify the created feature set. The classification performance reveals that the UV characteristics of these tissues are promising for correct identification of nervous fibers.

This article is organized as follows. In Chapter 2, materials used in this study are explained, and the SVM classifier is briefly explained in Chapter 3. Chapter 4 comprises the application and results of the study, and Chapter 5 concludes the paper.

2. Materials

In this study, nervous fibers, blood vessels, and muscles of two -year-old male cows were obtained from a meat supplier. From each animal, one piece of nervous fiber, blood vessel, and muscle tissue were taken and veterinarian of the butcher oversaw this process. Samples were placed on ice after recovery to avoid deterioration during transit to the laboratory. The number and type of each sample, along with the location from where they were obtained, is given in Table 1.

Light reflectance measurements of samples were carried out using a UV-NIR-SPM unit in the Bio-Nano Research Center of Fatih University. A snapshot from the unit is given in Figure 1(a). The UV-NIR-SPM unit can measure absorption, transmission, and reflectance spectra of light. Samples are first prepared for analysis by adjusting the size of each to fit the UV-NIR-SPM unit. All samples are prepared in similar shape and almost equal dimensions to minimize the effect of the geometry of samples on the measurement. These samples are prepared in the shape of a rectangular prism. The length of each sample is about 10 mm. the width and the thicknesses are 5 mm and 4 mm, respectively. Sample does not cover the whole sample stage window. The lamella used in the study is 45 mm long and 15 mm wide. Figure 1(b) shows a snapshot from some prepared samples for analysis.
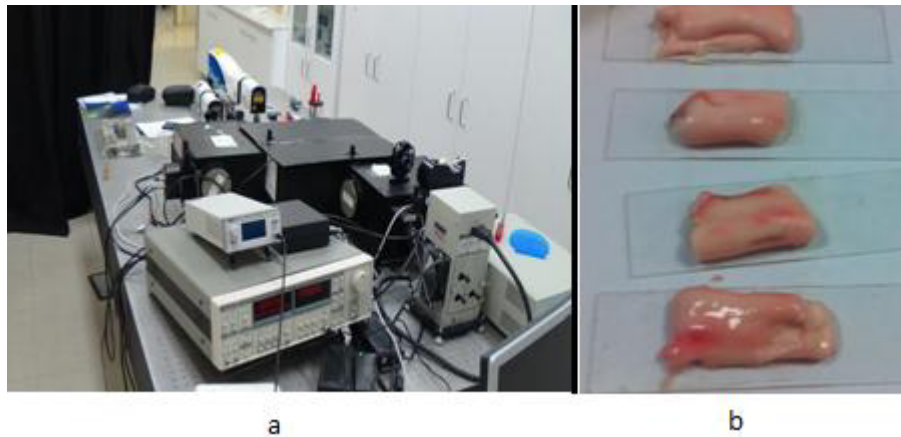
3. Support vector machine

Fig. 1. UV-NIR-SPM unit (a) and some samples ready for analysis (b).

The SVM is a supervised classification method widely used in different fields [14-16], including in classification problems that are linear and non-linear. It can be used for both two-class as well as multi-class classification problems [17, 18]. The classes used during classification are differently labeled. SVM draws an N-dimensional hyper plane, called a decision boundary [19], between classes. Supervised classifiers have two steps: training and testing. The feature set is divided into training and testing groups, and in the training phase the classifier learns the problem. This training set is fed into the classifier with known class labels, and the classifier arranges the weights of internal bounds that link features to the given label. The iterative learning process finishes with different criteria [20, 21]. The aim of the training phase is to calculate the decision boundary in an optimal way that lies midway between the adjacent classes. The functional margins must be maximized here to minimize the so-called generalization error [22]. At the end of the training step, the decision boundary is calculated and fixed. In the testing step, testing dataset is fed into the classifier without class labels. Then the system is asked to classify these datasets with the decision boundary obtained in the previous step. The classification performance is calculated according to the ratio of correct and incorrect classified samples.

4. Application and results

Samples of three kinds of tissues are taken from the butcher and each of them is analyzed with the UV-NIR-SPM unit. The light reflectance characteristics of each wavelength from 230 nm to 1000 nm are measured and tabulated. In the third step, the vulnerable wavelengths that can help to identify nervous fibers are determined. Then, the features are created in these wavelengths. These features are classified by using SVM classifiers. Finally, the classification performance is evaluated.

The UV-NIR-SPM unit has three basic components: a 500 watt Xenon Arc Lamp housing (Model XS 433, Acton Research Cooperation, 15 Discovery Way, Acton, MA), a monochromator (Princeton Instruments Acton Advanced SP 2300A), and a photomultiplier tube (PMT) (Hamamatsu H8259-01). The reflection measurement procedure is described below:

(1) White light from the Xenon lamp is sent to the sample that is to be measured.
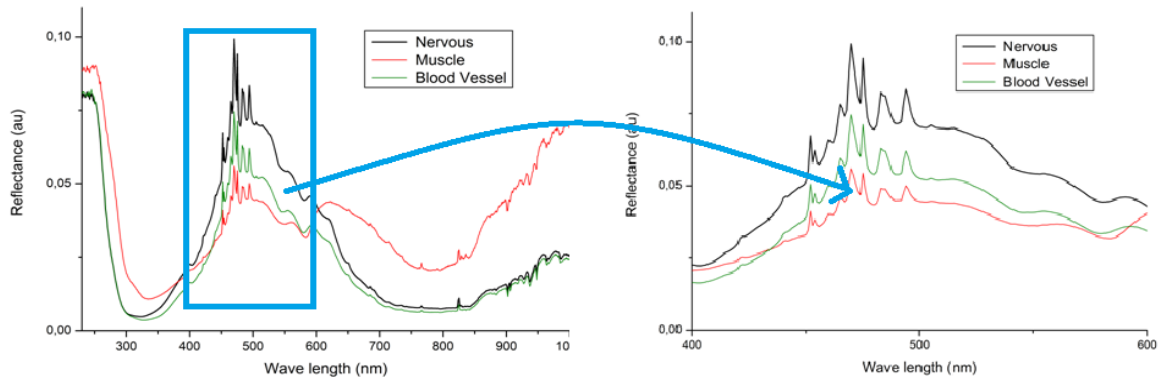(2) Reflected light is directed from the monochromator to the PMT to decide the wavelength of the light.

Fig. 2. Average value of tissues for 230 nm – 1000 nm (a) and focus on the vulnerable wavelength range (400 nm – 600 nm) (b).

(3) The reflectance of the given wavelength is measured.

(4) This procedure is repeated for each wavelength from 230 nm to 1000 nm.

A calibration process was carried out before actual samples are analyzed. For this purpose, a quartz mirror was used instead of the sample to provide full reflection. Thus, the full reflectance of the desired range (230 nm -1000 nm here) was measured (I_0). Then, each sample was placed and measured to obtain their spectrum (I). Finally, the process was normalized by taking the ratio of I/I_0.

In Figure 2(a), average values of each tissue type according to wavelength are given. The following can be summarized from this plot:

(1) For wavelengths lower than 300 nm, both blood vessels and nervous fibers show almost the same characteristics. The reflectance of muscle fibers is clearly higher than those of the other two for this wavelength range.

(2) After 300 nm, the reflectance of nervous fibers is different from the blood vessels, and it starts to increase with a higher slope.

(3) Around 380 nm, the reflectance of the nervous fibers reaches that of the muscle. Until 600 nm, the reflectance of the nervous fibers is the highest among the three.

(4) After 600 nm, the muscle has the highest reflectance. The reflectance of nervous fibers is still higher than that of blood vessels but the difference diminishes with the increasing wavelength.

(5) From this plot, the 400-600 nm interval seems to be the most vulnerable wavelength range for the correct classification of nervous fibers. In Figure 2(b), a zoomed view of the plot to the 400-600 nm range is given.

As explained in the previous section, the most vulnerable range of wavelength is 400-600 nm. Thus the classification features are extracted from this wavelength interval. In order to have robust features, four parameters are calculated for each of the 50 nm range. These parameters are minimum value, maximum value, average value, and the standard deviation. These values are calculated for 401-450, 451-500, 501-550, and 551-600 nm intervals. In other words, 16 features in total are calculated and the feature set is created.

In the previous literature, the k-fold cross-validation technique is frequently used to evaluate the performance of a classifier [23]. Here, the whole feature set is divided into k subsets. One subset is chosen as a testing feature set and the remaining k-1 subsets are used to construct the training feature set. The classifier is then allowed to run and the performance is recorded. In the next iteration, another subset is chosen as a testing feature set and the remaining k-1 feature sets are used to construct the training feature set. The performance of this iteration is also recorded. This procedure is repeated k

times. Then, the average performance of these iterations is calculated as the performance of the classifier. In this study, 10-fold cross-validation is chosen as it is widely used [24].

The feature set has two classes: nervous fibers and others. In other words, muscle and blood vessel samples are labeled in one class as our objective is to design a classifier that can distinguish nervous fibers. Then, 10-fold cross-validation is applied to a two-class classification problem. For each such iteration, performances are recorded and the overall performance is calculated by taking the average of 10 iterations.

The performance of a classifier can be defined by using sensitivity, specificity, and accuracy values. These parameters are calculated by the following formulae [25]:

- Accuracy

$$Accuracy = \frac{TP + TN}{N} \times 100(\%) \tag{1}$$

- Sensitivity

$$Sensitivity = \frac{TP}{TP + FN} \times 100(\%) \tag{2}$$

- Specificity

$$Specificity = \frac{TN}{TN + FP} \times 100(\%) \tag{3}$$

where,
- TP (True Positive): A nervous fiber is classified correctly.
- TN (True Negative): A non-nervous tissue is classified correctly.
- FP (False Positive): A non-nervous tissue is classified incorrectly as a nervous fiber.
- FN (False Negative): A nervous fiber is incorrectly classified as a non-nervous tissue.

Table 2

Classification results using SVM for 10-folds

Fold	# Support vector	C	Training Accuracy (%)	Test Accuracy (%)	Test Sensitivity (%)	Test Specificity (%)
1	13	0.5	100	100	100	100
2	15	0.5	100	100	100	100
3	13	0.5	100	100	100	100
4	14	0.5	100	100	100	100
5	14	0.5	100	100	100	100
6	11	0.5	100	100	100	100
7	14	0.5	100	100	100	100
8	13	0.5	100	100	100	100
9	12	0.5	100	100	100	100
10	14	0.5	100	100	100	100
Average			100	100	100	100

In Table 2, the performance of the 10-fold SVM classification is given. All folds give the highest accuracy, sensitivity, and specificity. Here, we can see that nervous fibers are classified from muscles and blood vessels with a high accuracy.

The nervous fiber, blood vessel and muscle tissue have different histologic structures. For example a nerve fiber is surrounded by a special kind of protein to enhance transmission of electrical impulse to its target organ, called mylein. A blood vessel is a tube shaped elastic structure to deliver blood to the end organs. A muscle tissue is comprised of actin and myosin to give strength. Therefore, all these tissues have different structures and densities that leads to difference reflectance of these tissues. However, the actual reason of the different reflactances are complicated to explain with a few causes.

5. Conclusion

This article is part of a research project to find structural properties that distinguish nervous fiber from blood vessels and muscles during surgery. Here, some structural properties of these tissues with different characteristics are investigated.

Three types of tissues were obtained from slaughtered cows. Their reflectance with respect to wavelengths of light was examined by using a UV-NIR-SPM unit. The reflectance of each sample was measured in a large range (230 – 1000 nm). Graphical investigation revealed that the 400-600 nm range is very vulnerable when differentiating nervous fibers from the other two types. Then, classification features were created for this range and the SVM classifier was utilized to make an automatic classification. The output of the classifier was significant.

The light reflectance of these tissues for the 400-600 nm wavelength range can be used to establish a real life instrument that can be used in surgery.

Acknowledgment

References

[1] T.E. Dominguez, G. Wernovsky and J.W. Gaynor, cause and prevention of central nervous system injury in neonates undergoing cardiac surgery, Seminars in Thoracic and Cardiovascular Surgery **19** (2007), 269–277.

[2] P. Rea, Introduction to the nervous system, in: Essential Clinical Anatomy of the Nervous System, P. Rea, ed., Academic Press, San Diego, 2015, pp. 1–50.

[3] L. Deng, C. Walker and X.-M. Xu, Schwann cell-mediated axonal regeneration in the central nervous system, in: Neural Regeneration, K.-F. So and X.-M. Xu, eds., Academic Press, Oxford, 2015, pp. 337–349.

[4] S.H. Woo, et al., Comparative analysis on the efficiency of the injection laryngoplasty technique using calcium hydroxyapatite (CaHA): The thyrohyoid approach versus the cricothyroid approach, Journal of Voice **27** (2013), 236–241.

[5] M. Schumacher, et al., Revisiting the roles of progesterone and allopregnanolone in the nervous system: Resurgence of the progesterone receptors, Progress in Neurobiology **113** (2014), 6–39.

[6] A.M. Hopkins, et al., 3D in vitro modeling of the central nervous system, Progress in Neurobiology **125** (2015), 1–25.

[7] J. Mingo-Robinet, et al., Tourniquet-related ıatrogenic femoral nerve palsy after knee surgery: Case report and review of the literature, Case Reports in Orthopedics **2013** (2013), 4.

[8] H. Dralle, et al., Intraoperative monitoring of the recurrent laryngeal nerve in thyroid surgery, World Journal of Surgery

32 (2008), 1358–1366.

[9] G. Gremillion, et al., Intraoperative recurrent laryngeal nerve monitoring in thyroid surgery: Is ıt worth the cost? The Ochsner Journal **12** (2012), 363–366.

[10] G.W. Shaftan, How interventional radiology changed the practice of a trauma surgeon, Injury **39** (2008), 1229–1231.

[11] A.R. Moller and P.J. Jannetta, Preservation of facial function during removal of acoustic neuromas, use of monopolar constant-voltage stimulation and EMG, Journal of Neurosurgery **61** (1984), 757–760.

[12] G.W. Randolph, et al., Electrophysiologic recurrent laryngeal nerve monitoring during thyroid and parathyroid surgery: International standards guideline statement, Laryngoscope **121** (2011), S1–16.

[13] Y.A. Ashram, et al., Intraoperative electrophysiologic identification of the nervus intermedius, Otology & Neurotology **26** (2005), 274–279.

[14] K. Tufan, Noninvasive diagnosis of atherosclerosis by using empirical mode decom-position, singular spectral analysis, and support vector machines, Biomedical Research **24** (2013), 303–313.

[15] Z. Liu, et al., A time-sequence-based fuzzy support vector machine adaptive filter for tremor cancelling for microsurgery, International Journal of Systems Science **46** (2015), 1131–1146.

[16] J. Chai, et al., A hybrid least square support vector machine model with parameters optimization for stock forecasting, Mathematical Problems in Engineering **2015** (2015), 231394.

[17] A. Airola, T. Pahikkala and T. Salakoski, An ımproved training algorithm for the linear ranking support vector machine, Artificial Neural Networks and Machine Learning **6791** (2011), 134–141.

[18] P.P. Bing, S.Y. Cao and J.T. Lu, Non-linear AVO inversion based on support vector machine, Chinese Journal of Geophysics **55** (2012), 1025–1032.

[19] F. Camci and R.B. Chinnam, General support vector representation machine for one-class classification of non-stationary classes, Pattern Recognition **41** (2008), 3021–3034.

[20] O. Medelyan, et al., Mining meaning from Wikipedia, International Journal of Human-Computer Studies **67** (2009), 716–754.

[21] P.G. Zimbardo, Discontinuity theory: Cognitive and social searches for rationality and normality—may lead to madness, in: Advances in Experimental Social Psychology, P.Z. Mark, ed., Academic Press, San Diego, CA, US, 1999, pp. 345–486.

[22] M. Dätig and T. Schlurmann, Performance and limitations of the Hilbert–Huang transformation (HHT) with an application to irregular water waves, Ocean Engineering **31** (2004), 1783–1834.

[23] S. Ounpraseuth, et al., Estimating misclassification error: A closer look at cross-validation based methods, BMC Research Notes **5** (2012), 656.

[24] Q. Noirhomme, et al., Biased binomial assessment of cross-validated estimation of classification accuracies illustrated in diagnosis predictions, NeuroImage: Clinical **4** (2014), 687–694.

[25] M.S. Jadin , S. Taib and K.H. Ghazali, Feature extraction and classification for detecting the thermal faults in electrical installations, Measurement **57** (2014), 15–24.